The colours of the extreme universe

Calistro Rivera, G.

1

Introduction

1.1 The Building Blocks of the Observable Universe

You are reading these lines on some spot on Earth, one of the eight planets that orbit our closest star, the Sun. The Sun is in turn one element in a structure of a few hundreds of billions of stars[1] bound by gravity and defined as a galaxy, our galaxy, the Milky Way. Such as the Milky Way, trillions of galaxies[2] of a large diversity of sizes, shapes and masses are the building blocks of our vast observable Universe. The exploration of the observable Universe is an endeavour inherent to the human nature and thus from ancient times human civilizations have targeted their skills and imagination to observe and map the skies. However, the scientific study of the observable Universe has seen an unprecedented development only recently, after the telescope constructed by Galileo Galilei evolved, hand in hand with technology, into magnificent machines of exploration. These machines do not only deepen our view to look into inconceivable distances, but also broaden the spectrum allowing us to see and understand the Universe through colours not even humanly perceivable. In this thesis we will make parallel use of most kinds of these machines and portray the early Universe at different colours. We will show how the study of the panchromatic emission of galaxies will provide us with a more complete physical understanding of the extreme and distant Universe.

Galaxies beyond our own and their central black-holes

The existence of other galaxies beyond our own, and extragalactic astronomy as such, is a concept that first came into inception no more than hundred years ago. In the 1920s, using the new 100 inch Mt. Wilson optical telescope, Edwin Hubble confirmed that many of the nebulae or clouds reported by previous observations were too distant to belong to our own galaxy. This was the final remark in a long and complex path of this discovery of a extragalactic Universe. As most breakthroughs in astronomy, this discovery was a long process, involving a large number of observations (such as the 'nebulae' catalogs of Charles Messier and William Herschel) and centuries of debate, to finally confirm the nature of these nebulae as extragalactic objects.

E. Hubble himself would then portray the morphological diversity of galaxies through a classification scheme used till today, which divides galaxies into spirals, ellipticals and irregulars. Soon after, it would be discovered that observing galaxies with two or more colour filters, and comparing the different measurements in a magnitude-colour diagram, could separate them principally into blue and red galaxies. Blue galaxies being galaxies actively growing through the formation of stars, and red galaxies having primordially old stellar populations, undergoing a quiescent state with no significant star formation. Later on, observing the skies with telescopes that probe different parts of the electromagnetic spectrum of light, new galaxy

[1] GAIA DR2 (Gaia Collaboration et al. 2018)
[2] Conselice et al. (2016)

populations would be discovered, entirely invisible or barely detectable at optical wavelengths, revealing the complexity and panchromatic nature of galaxies.

The first evidence that some galaxies were hosting highly-luminous nuclei in their centers was found in the 1940s by Carl Seyfert, when he detected unexpectedly bright and broad emission lines in the central regions of nearby galaxies (Seyfert 1943). Around 20 years later, the discovery of enigmatic quasi-stellar radio sources (quasars) using optical spectra and radio continuum observations (e.g., Schmidt 1963), would then revolutionize our notion of galaxies. These observations put forward the concept that the large nuclear luminosities observed in these galaxies were produced by massive nuclear black-holes feeding matter and growing through a luminous accretion process. Later observations would then show that most galaxies, if not all, host massive black holes in their centres (Lynden-Bell 1969), a concept that represents now one of the pillars of extragalactic astronomy. Indeed, a strangely immobile radio source, of a luminosity similar to our own Sun, would be discovered some years later in the center of our own galaxy revealing that even our own Milky Way hosted a massive black hole in its centre, which was called Sagittarius A* (Lynden-Bell & Rees 1971). The fact that the Sagittarius A* galactic nucleus is a weaker radio/ X-ray source by 5–10 orders of magnitude[3] than the earlier discovered quasars would also demonstrate the existence of a large variety of galactic nuclei. Indeed, while most galaxies host massive and super-massive black holes in their centers, these are experiencing different activity levels.

This thesis focuses on characterizing the most extreme epoch of cosmic history, where most of galaxy growth took place. As will be discussed in detail in Section 1.3, growing BHs are ubiquitous in the centers of galaxies populating this period. Indeed, one of the most important discoveries around galaxies and their active galactic nuclei is the finding of a tight correlation between the masses of the galaxy spheroids and those of the central black holes in the local Universe (e.g., Kormendy & Richstone 1995; Magorrian et al. 1998; Marconi & Hunt 2003; Gültekin et al. 2009). While this finding suggests a symbiotic relation between the host galaxy and its central nucleus, this is a surprising observation due to the extremely different scales inhabited by host galaxies and black holes: the stellar and gas content in a galaxy is distributed on scales of $1-100$ kpc, while the black-hole accretion occurs only on scales of < 1 pc. These observations suggest that physical mechanisms should be in place which transport gas onto those small scales. However, these mechanisms are still not understood and the galaxy-black hole co-evolution remain an intriguing question that sparkles lively discussions in the astronomical community.

The formation of stars in the Universe appears to be very inefficient if we notice that the fraction of baryons which make up stars and stellar remnants in the present day Universe has been observed to be $< 6\%$ of the total baryon content of the Universe (e.g., Fukugita & Peebles 2004). The large radiative energies emitted in the process of black hole accretion place quasars and other active galactic nuclei as the most probable candidates to be the regulators of galaxy growth. This occurs through feedback processes that heat or expel the gas from the interstellar medium of galaxies, preventing the formation of stars. Cosmological simulations (e.g., EAGLE, IllustrisTNG), which use numerical recipes to mimic galaxy formation and evolution from the Big Bang till the present day, use this 'AGN feedback' in order to calibrate the cosmic star formation history of the Universe, so that it matches the observed present-day stellar content. Understanding the co-evolution of galaxies and AGN is thus a crucial element to characterize the build-up of matter in the Universe.

[3] Sgr A* has a bolometric luminosity of less than $L_{bol} = 10^{37}$ erg s^{-1}

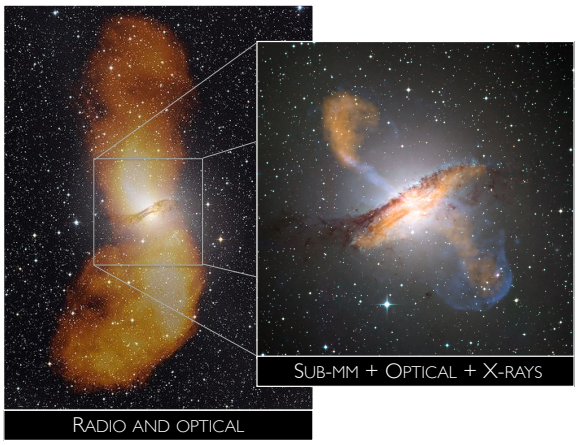

Figure 1.1: Multiwavelength emission of the galaxy NGC 5128, known as Centaurus A. The *left panel* shows a composition of the radio emission of the outer-lobes extending ∼a million light-years from the galaxy and the optical galaxy emission. (Credit: Capella Observatory (optical), CSIRO/ATNF, ASTRON, MPIfR (radio)). The *right panel* shows a zoom-in view on the inner-lobes and the central galaxy, as a composition . of sub-mm, X-ray and optical emission (Credit: ESO/A. Weiss et al.; NASA/CfA/R.Kraft)

Observing galaxies and black-holes across cosmic time

Light is the main source of information when observing galaxies in the Universe. Any description that involves distances travelled by light and time scales over a significant fraction of cosmic time, including the age of the Universe, are highly dependent on the cosmological framework chosen. The current standard model of Big Bang cosmology is the Λ-cold dark matter model (ΛCDM). ΛCDM prescribes the formation of structure in the Universe based on the equations of general relativity (Einstein 1916), while being able to explain the observed early structure formation imprinted on the cosmic microwave background (Planck Collaboration et al. 2014). Based on ΛCDM, the energy content in the Universe is dominated by dark energy (69.2%, parametrized by Λ) and cold dark matter (26.8%), while baryons represent only 4%, from which only 6% are visible. While dark matter is a form of matter that interacts with baryonic matter only through gravity, dark energy is the cosmological constant that determines that the Universe is expanding in an accelerated manner, as confirmed by observations (Riess et al. 1998; Perlmutter et al. 1999),

The constant speed of light at $c = 3 \times 10^8$ m s^{-1} is of great value to galaxy evolution studies since it allows us to look back in time. Due to its constant velocity, light produced at early times of cosmic history would reach us only now, allowing us to witness these early events. Additionally, light travelling towards us is 'stretched' to longer wavelengths by the expansion of the Universe, in a phenomenon call redshift. The accelerated expansion of the Universe produces a redshift that is higher at earlier epochs, serving as a tag for the time when an event has occurred. For instance, the galaxy NGC 5128 shown in Figure 1.1, better known as Centaurus A, is one of the closest radio AGN to us and is located at a distance 3.8 ± 0.1 Mpc (Harris et al. 2010).To arrive to us from that distance, light has travelled ∼ 10 million years (10 Myr). Since this is a negligible amount of time, compared to the age of the Universe (13.8 Gyr from the Big Bang), Centaurus A is at redshift $z \sim 0.0006$. The light of a galaxy observed at redshift $z = 2$ – the median redshift of the galaxies studied in this thesis – would have travelled towards us for 10.5 Gyrs; and at redshift $z = 4$, only 1.5 Gyrs had passed since the Big Bang.

Albeit the emission we can observe from Centaurus A has originated fairly 'recent', the formation and evolution of that galaxy is expected to have started > 10 Gyr ago, based on

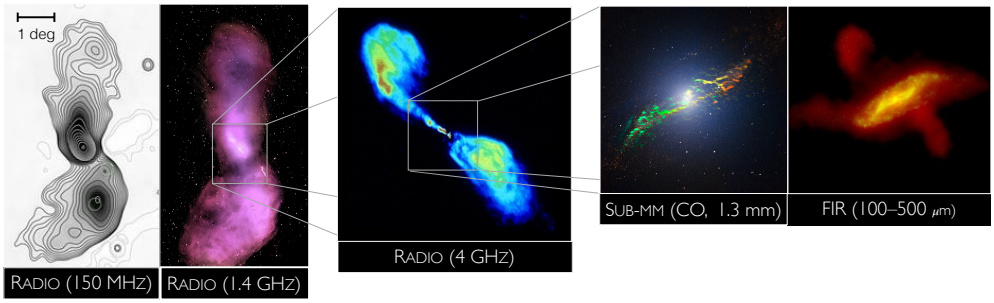

Figure 1.2: Multiwavelength radio–infrared emission of Centaurus A. Credit: PAPER array, Stefan et al. 2013(150 MHz), Morganti et al. 1999, Feain et al. 2011 (1.4 GHz), VLA Burns & Price, 1983 (4 GHz), ALMA/ESO (sub-mm), ESA/Herschel/PACS/SPIRE/C.D Wilson (FIR)

theoretical modelling of the stellar populations in its halo (Rejkuba, M. et al. 2011). Indeed, due to the cosmological time scales implied in the formation and life-time of a galaxy, it is impossible for humans to directly follow galaxy evolution. To characterize galaxy evolution through observations, astronomers thus require large unbiased samples of galaxies populating different epochs across cosmic time. Observing galaxies at different redshifts would then allow us to connect galaxy populations (of similar fundamental properties) across a single evolutionary path in order to test theoretical evolutionary models. However, most methods used to study galaxy evolution are limited by properties of light that need to be taken into account. The intensity of light decreases as a function of the inverse square of the luminosity distance it has travelled towards the observer, where the luminosity distance is a function of $\propto (1+z)^{-2}$. This implies a decrease of the flux density as measured by instruments of $\propto (1+z)^{-4}$. It is thus challenging to detect the most distant galaxies at earlier epochs, largely biasing galaxy samples to contain only the most luminous galaxies. Since most observational campaigns can sample only the most luminous and thus massive galaxies across all redshifts, *the most extreme sources are an ideal laboratory to trace galaxy evolution.*

Similarly, the observed angular sizes of galaxies decreases as a function of the inverse square of the distance, preventing the angular resolution of current instruments from resolving the detailed morphology of the sources. Additionally, high-resolution observations need to detect low-surface brightness emission and thus require larger exposure times and become highly expensive. The advent of recent and future high-resolution and sensitivity telescopes, such as the Hubble Space telescope (*HST*), the Atacama Large Millimeter Array (*ALMA*) and the mid-infrared James Webb Telescope (*JWST*), will make it possible to study galaxy evolution from a resolved perspective. In this thesis we will present some exceptional examples of high-resolution multiwavelength studies using these new-generation instruments.

The emission of a galaxy across the electromagnetic spectrum is very complex since a large variety of physical processes, probing different spatial scales, contribute simultaneously to the emission. Observations from single telescopes at given wavelengths are thus always biased for or against certain properties or structured within galaxies, as can be seen in different views of Centaurus A achieved across the electromagnetic spectrum in Figures 1.2 and 1.3. Moreover, the emission of some galaxy populations at given redshifts might be so weak at certain wavelengths that they would remain entirely undetected in these observations. Observing galaxies at single wavelengths, even when these are detectable, is thus commonly not enough to understand the physics or the initial conditions producing the emission. *Multiwavelength approaches are thus essential to have a full description of galaxy physics.*

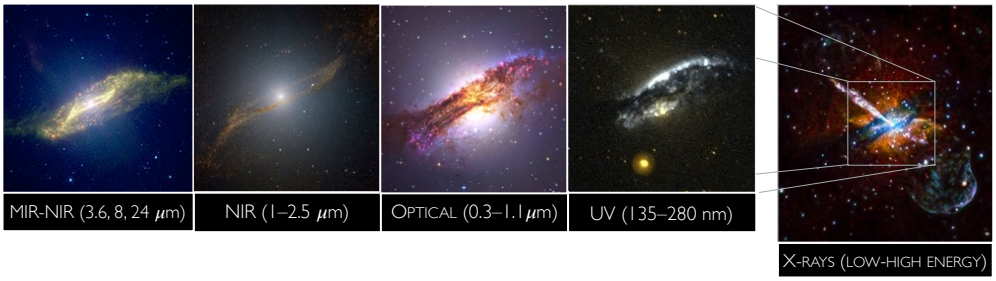

Figure 1.3: Multiwavelength infrared–X-rays emission of Centaurus A. Credit: IRAC(at 3.6 and 8 μm) and MIPS (24 μm)/Spitzer/NASA-JPL (mid-infrared); J, H and K bands, SOFI at NTT/ESO (near-infrared); NASA/ESA/STScI/ESO/Robert Gendler/Roberto Colombari (optical); NASA/Chandra X-ray Observatory (X-rays).

1.2 The Panchromatic Nature of Galaxies and AGN

Figures 1.2 and 1.3 illustrate the different views of the radio galaxy Centaurus A (star forming and AGN), achieved observing at some of the parts of the electromagnetic spectrum covered by this thesis. In Centaurus A, structures probed at different wavelengths can be characterized in detail, since this source is one of the closest and brightest galaxies in the Universe. For galaxies at redshifts $z \sim 2$, however, resolving any galaxy structure becomes almost impossible at these wavelengths using current instruments (see exceptional cases in Chapter 4 and 5 of this thesis). Fortunately, integrated emission averaged across the entire galaxy can provide valuable insight on the properties of sources in the early Universe when combined with theoretical models.

A representation of the complexity of the electromagnetic spectrum emitted by galaxies can be achieved through the sampling of the galaxy's spectral energy distribution (SED). The SED is the distribution of energy over frequency or wavelength and is usually constructed using broadband photometric observations of a galaxy across the spectrum. All physical processes responsible for the radiative emission of galaxies, including those from the galactic nuclei, are imprinted in the shape of the SED. Historically, early versions of SED models were mostly limited to fitting stellar emission in the UV-NIR regime (e.g, Bolzonella et al. 2000; Brinchmann & Ellis 2000). The last decade has seen significant development in the modelling of other parts of the spectrum providing SED-fitting approaches that model the infrared and radio regimes as well (e.g., Burgarella et al. 2005; da Cunha et al. 2008). In Figure 3.4 we summarize the panchromatic emission of galaxies that has been studied in this thesis. Below, we describe the physics behind the integrated panchromatic emission of galaxies, starting from the high-energy regime (X-rays) to the low-energy end (radio) of the spectrum covered by this thesis.

High energy black-hole physics: optical, UV and X-rays

The **optical/UV** regime of the integrated SED of a galaxy hosting an AGN is typically dominated by the nuclear emission. This is a product of the *accretion of gas* onto the gravitational potential of its central massive black hole. An optically thick accretion disk of material (Shakura & Sunyaev 1973) is formed as the black hole grows, producing a luminous and broad thermal continuum emission at temperatures around 105 K, commonly known as the "big blue bump". The observed shape of the accretion disk SED is further altered by dust attenuation at

nuclear or galactic scales. While its integrated emission is prominent, the accretion disk is too small to be spatially resolved even in local galaxies since it is expected to surround the black-hole at scales of around few light-days for local Seyfert and less than a few light-years for quasars. Apart from the continuum, the nuclear optical-UV emission is also characterized by the presence of broad (∼1000 km/s) and narrow (300–1000 km/s) emission lines, originated from gas clouds distributed at scales of less than 1 and a few hundred pc around the accretion disk, respectively. In bright star-forming galaxies, with weak or highly obscured AGN, the optical-UV part of the SED can be dominated by the emission of stellar populations as will be discussed below. Surrounding the accretion disk, a corona of hot electrons is responsible for the intrinsic **X-ray emission** through *inverse Compton scattering of the accretion disk UV-photons*, producing a power-law shaped X-ray continuum. This intrinsic emission is then altered by the interaction with other nuclear components, such as photo-electric absorption, reflection and scattering. The X-ray emission in most galaxies is dominantly originated in the AGN and is thus often used as one of the most reliable AGN tracers and the largest and arguably less-biased AGN surveys have been selected based on detections in X-ray surveys (see Brandt & Alexander 2015, for a review). However, as X-ray surveys go deeper, the weak X-ray emission detected starts tracing the weak emission of stellar X-ray binaries that are X-rays luminous, contrary to the majority of stellar populations.

The stellar emission: NIR, optical and UV

Historically, the most studied part of the galaxy SED is the **near-infrared, optical and UV** emission emitted by the *stellar populations* that compose the galaxy. The stellar SED is shaped by the physical properties of the stellar populations composing the galaxy, including the star formation history, the metal content in stars, the dust distributions and the interstellar radiation. The galaxy SEDs are commonly studied using stellar population synthesis modelling, which rely on stellar evolution theory to determine the ensemble of possible stellar types at a given age and metallicity that is needed to explain the shape of the SED (see Conroy 2013, for a review.). The building blocks of such a model are Simple Stellar Populations (SSP), which are single populations of stars of equal metallicity and undergoing equal stellar evolution. The 'mock' galaxy emission from a SSP is produced as a superposition of empirical and theoretical stellar spectral libraries following the distribution dictated by an assumed initial mass function (IMF). The total galaxy stellar SED is then constructed as the composite of different SSPs, of different ages and metallicities, as determined by the SFH and the metallicity evolution of the galaxy, respectively. Generally speaking, the blue end of the optical-UV emission of the stellar SED is then dominated by the emission of young stellar populations of recent star formation. The intensity of the blue end is thus largely determined by the star-formation history of the galaxy and is essential to *determine the star formation rate* of the galaxy in the optical/UV regime. The near-infrared end of the stellar SED, on the other side, is dominated by the reddest, more massive and oldest stars, being thus crucial for the *estimation of stellar mass* of the galaxy.

The intrinsic emission from the different stellar populations and the shape of the optical/UV SED can be largely attenuated and absorbed by dust distributions typical of star forming regions. This emission is reprocessed and re-emitted by the dust at infra-red wavelengths, as will be explained below. Dust attenuation is a determining factor for the capability of the optical/UV SED as a tracer of star formation, since corrections for dust attenuation can be uncertain, preventing robust measurement of the intrinsic young stellar emission. In contrast, the NIR part is less affected by obscuration and thus stellar masses are usually a fairly well-constrained quantity in SED-fitting (within a relative error of 0.1-0.2 dex, Muzzin et al. (2009)). However, although less discussed in the literature, the NIR emission of the stellar

population can be contaminated by the emission of nuclear host dust, when the galaxy host AGN. This emission can produce overestimated stellar masses when is not taken into account. This thesis will explore the effect of including AGN in the panchromatic modelling.

The hot nuclear dust and molecules at galactic scales: MIR

AGN can emit considerable fractions of their total energy output in **mid-infrared and near-infrared** wavelengths. This component originates in the nuclear obscuring material, composed of *hot gas and dust* at scales of few parsecs (e.g., Alonso-Herrero et al. 2011; Ichikawa et al. 2015), which is heated by the high-energy accretion disk emission. The obscuring material has been historically believed to be shaped in the form of a torus. Recent results suggest that a clumpy toroidal structure is a more accurate description (Nenkova et al. 2002), albeit the distribution is not well constraint due to the lack of observational evidence. The gas is the principal obscuring material of the X-ray part of the nuclear emission, and the dust attenuates mainly the optical-UV emission. This material is distributed closely around the accretion disk, at a distance defined by the sublimation temperature of dust, where dust grains and gas molecules can be formed. The morphology and orientation of this obscuring torus play an important role for the diversity of AGN. The presence or absence of broad-lines in the optical spectra of AGN, which classified them into type 1 and 2, respectively, is considered to be closely related to the viewing angle of the observer to the torus, whether it was face-on or edge-on, respectively. We will discuss AGN obscuration in detail in Chapter 2 of this thesis.

The MIR part of the SED of star forming galaxies and AGN is also characterized by hosting **poly-cyclic aromatic hydrocarbons (PAHs)** (e.g., Tielens 2008), which are large molecules emitting the brightest emission lines across the spectrum and are thus a prominent component of the MIR emission of galaxies. PAHs are abundant in galaxies with metallicities close to solar and since they typically populate star-forming regions in galaxies, they are usually used as tracers of star formation. Strong peaks that compose the feature complexes of PAHs can usually fall around $6-8\,\mu$m and $11.2-12.7\,\mu$m. Due to their large luminosities and widths, the PAH contribution and the strength of the hot dust continuum are parameters that are often degenerate, in particular when only broadband photometry is available. Degeneracies, correlations and other statistical challenges in the modelling of the multiwavelength SEDs will be investigated in Chapter 2 of this thesis.

The interstellar medium: FIR and sub-mm

The far-infrared and sub-millimeter regime in a galaxy's SED is dominated by the **continuum emission of cold dust** distributed in the interstellar medium of star forming regions. The emission originates in dust that is heated by the UV and optical stellar emission, in particular by the young and short lived stellar population of red giant stars. The FIR emission is thus an indirect indicator of the recent star formation and is used as a *reliable star formation rate tracer*. The FIR SED is a thermal emission, composed as a superposition of black-bodies at different temperatures whose shape is described by Planck's law. The temperatures of each black-body is determined by parameters such as the dust distributions around the heating source, and the size of the dust grains, where small grains are usually heated faster and produce higher-energy thermal emission than large grains. The total SED has then a characteristic peak that gives the mean temperature of the dust in the system, usually around 30-40 K (e.g., Casey et al. 2014), which is a characteristic temperature for the heating of molecular clouds by star formation activity. The low-energy, submillimeter end of the SED is consistent with the Rayleigh Jeans (RJ) tail, which provides the FIR SED with a remarkable property, the negative K-correction. A K-correction describes the change of the intensity at a given wavelength as

a product of redshift, since the SED shifts towards lower energies as the redshift increases. Since the shape of the RJ tail (positive slope) counteracts the flux density dimming by the increased distance to the observer (negative slope), the observed sub-millimeter flux density remains almost constant for galaxies at redshifts $1 - 8$ (Casey et al. 2014). This thesis benefits from this negative K-correction and studies the high-redshift Universe targeting sub-mmm-selected galaxies in Chapters 4 and 5.

The sub-millimetre regime of a galaxy's emission is also characterized by tracing the emission of **molecular and atomic gas** in the interstellar medium (ISM). Molecular gas is predominantly distributed in the ISM within molecular clouds of sizes up to 50 pc, as has been observed in the Milky way and nearby galaxies (e.g., Carilli & Walter 2013) The most abundant molecule in the ISM is molecular hydrogen (H_2), but is undetectable due to its lack of rotation-vibrational transitions. Carbon, on the other hand, does not only play an important role in the ISM as the main provider of free electrons, but provides some of the brightest emission lines in the sub-mm regime. The carbon monoxide molecule (CO) ($\sim 10^{-4}$ as abundant as H_2) and the fine-structure line of the carbon ion [C II] are among the main tracers of the molecular gas and the most luminous emission lines in the sub-mm, being able to contribute up to $20 - 40\%$ of the total sub-mm flux (Smail et al. 2011). Chapters 4 and 5 of this thesis studies the emission of these two lines at high-resolution in order to characterize the ISM in detail.

Interacting plasma: radio

The emission at intermediate and low radio frequencies (<10 GHz) is dominated by synchrotron emission. Synchroton emission is generally produced by the interaction of ultra-relativistic ($E \ll m_e\ c^2$) electrons with a magnetic field, in this case the magnetic field of the galaxy. The sources of accelerated electrons, or plasma, in galaxies are related to both AGN and star-formation processes.

In AGN, and specifically radio galaxies and radio quasars, immense relativistic collimated streams of plasma, called radio jets, are emitted from the accretion process of the black hole. These radio jets can extend to scales even larger than the host galaxy and the details around the origin and conditions in which these form are still open questions in astronomy. Historically, the low sensitivity of radio telescopes assured that these radio AGN with luminosities that can reach $P_{1.4\ \mathrm{GHz}} \sim 10^{27}$ were the only sources detectable at radio frequencies (thus the general nomenclature of 'radio galaxy'). The radio was thus used as a tracer of black hole activity.

However, the interstellar medium of galaxies is also pervaded of interstellar plasma, produces by the acceleration of electrons in supernova remnants. Since supernova remnants are direct products of the short-lived massive stars (with stellar masses of $M \leq 8\ M_\odot$), the interstellar synchroton emission is used as a tracer of recent massive star formation in galaxies. The interstellar synchroton emission, however, produces usually luminosities below $P_{1.4\ \mathrm{GHz}} \sim 10^{24}$, populating the low end of the radio luminosity function (Condon 1992; Padovani 2016). These luminosities have become detectable only recently, with the advent of radio interferometer such as the low frequency array (LOFAR), and star forming galaxies have been included in radio-selected galaxy samples only recently. A key property of radio emission from star-forming galaxies is that it presents a tight correlation with the far-infrared emission, also a tracer of star formation. This correlation is a fundamental instrument to disentangle the radio emission arising from the AGN to that from the galaxy, which are otherwise indistinguishable, since both have been observed to present a fairly similar SED simplied as a steep negative power-law with a spectral index of $\alpha \sim -0.7$. In this thesis we will explore in detail both the far-infrared radio correlation and the radio SED at low-frequencies (150 MHz) for the first time (Chapter 3). At high frequencies ($\nu > 30$ GHz) the radio emission in

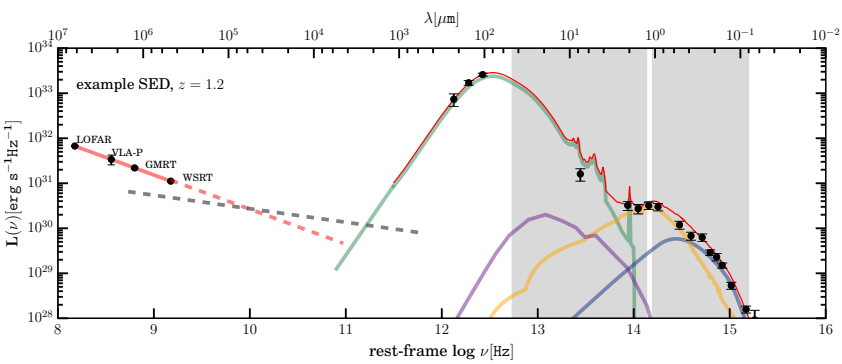

Figure 1.4: Example SED of dusty star forming galaxy at $z = 1.2$. The data points are representative of the photometric data covered in this thesis. The photometry is modelled and decomposed into physical components of the host galaxy and the AGN. The dashed red and grey lines correspond to the synchroton and thermal contributions to the radio emission, respectively. The green line corresponds to the FIR and sub-mm dust continuum emission from star forming regions, while the yellow line represents the NIR/optical emission from stellar populations. The purple line represent the hot dust emission from the nuclear obscuring medium or 'torus'. Finally the blue line represents the accretion disk emission of the AGN, attenuated by obscuration. The thin red line represents the total fitted SED.

star forming galaxies starts to be dominated by a thermal flat free-free component, which isc directly related to the rate of ionizing photons arising from newly formed massive stars. This part of the spectrum, however, is outside the scope of this thesis.

1.3 The Epoch of Extreme Galaxy and Black-hole Growth

Based on observations across the electromagnetic spectrum of light, fundamental properties have been learned and new questions have been posed about the nature of galaxies and black holes. Galaxies grow through the transformation of gas (mostly molecular) into stars, and indeed, the star formation rate (SFR) and the stellar mass are the main integrated properties that describe the evolutionary state of a galaxy. Efforts to characterize galaxy evolution have demonstrated that the position of a galaxy on this sequence, or the specific star formation rate (sSFR), is a fundamental property and decisive for the galaxy's fate. Based on these properties, studies have found that most of star-forming galaxies at a given redshift follow a '**main sequence**' (Brinchmann et al. 2004; Whitaker et al. 2012), which is defined as a relatively tight distribution (<0.3 dex) in star formation rate versus stellar mass. Although this relation evolves as a function of redshift, where main sequence galaxies at a fixed mass present higher SFR at higher redshifts, a main sequence is found to exist at both low and high redshifts. Indeed, the star formation rates of some of the most massive main sequence galaxies in the early Universe can reach values up to a few 100 $M_{\odot}yr^{-1}$.

The total **cosmic star formation history of the Universe** can be characterized based on the integrated properties measured for large samples of galaxies selected across the spectrum, and on unresolved measurements of the cosmic background at different wavelengths. A key finding was that both, the cosmic star formation history and BH evolution evolves as a function of redshift, increasing from the local Universe towards the past, peaking at redshifts $z \sim 2$, when the Universe was 3 Gyrs old, declining again at earlier epochs (See Figure 1.5). This

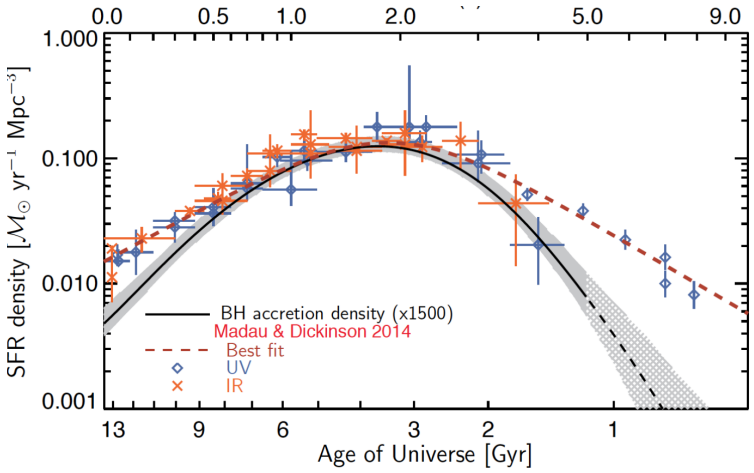

Figure 1.5: Co-evolution of galaxies and black holes. Adapted from Aird et al. (2015). The dots represent the observed SFR density per unit volume versus cosmic time using the tracers indicated in the legend. The dashes line indicates the best fitting relation to these observations (Madau & Dickinson 2014). The solid line shows the accretion rate density from observations of X-ray selected AGNs (Aird et al. 2015), re-normalized by a factor of 1500. The peak and shape of the distribution of both the SFR and accretion rate densities across cosmic time show a remarkable similarity.

epoch of galaxy assembly – which is the focus of this thesis – represents a key phase of galaxy evolution, since most of the stars in the present day Universe are believe to be formed in this phase. Furthermore, the observation that the peaks of both processes are coincidental is a strong support for the tight galaxy-BH co-evolution scenario, and suggest that this epoch is a good laboratory for the study of the apparent symbiotic and enigmatic relation between the galaxies and their nuclei.

Based on observations of galaxies and AGN at this epoch, the **probability of finding AGN in the centers of star forming galaxies** has been studied extensively (Kirkpatrick et al. 2012; Rosario et al. 2013, 2015; Aird et al. 2018). Clearly, the AGN fraction within a galaxy population depends strongly on the wavelength of selection and flux limits probed. Selections at wavelengths where the AGN features in the SED are more prominent, such as the MIR, UV and X-rays (Figure 3.4), would deliver larger AGN fractions than other regimes, where galaxy emission dominates. Another important factor that affect the probability of finding a luminous AGN hosted by a galaxy is the different time-scales probed by star formation and BH accretion, since AGN activity can vary by a factors of $\sim 0.1 - 1$ Myr timescales (Volonteri et al. 2015), whereas star formation time scales can achieve time scales of a few Gyr. Remarkably, recent unbiased studies of mass-selected samples of galaxies have shown that the probability of finding significant emission originated in AGN accretion increases as a function of stellar mass, star formation rate and redshift (Fig. 1.6, e.g. Aird et al. (2018)). In particular, at $z \sim 2 - 3$ – on which this thesis is focused – the probability of black hole growth within galaxies at all masses and star formation rates achieves its peak. The ubiquity of accreting black holes in highly star forming galaxies is thus an important factor to take into account, even for galaxy populations with emission dominated by star formation.

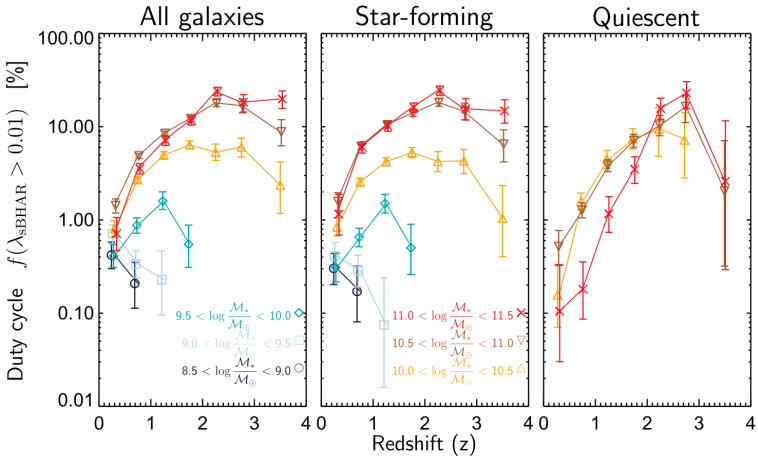

Figure 1.6: The evolution of the fraction of galaxies hosting AGN (duty cycle) as a function of redshift, stellar mass, and SFR. From Aird et al. (2018).

An extreme and obscured epoch

A key finding that revolutionized our understanding of galaxy evolution was that an important fraction of the star formation occurring during this epoch is invisible to optical wavelengths since it is enshrouded by dust. Most critically, observations of the COsmic Background Explorer (COBE) revealed that the cosmic extragalactic background at infrared wavelengths was comparable to that at optical wavelengths. This was a strong suggestion that around half the extragalactic emission, originated from galaxies and AGN, must be enshrouded by dust. Indeed, later observations with the Herschel telescope would confirm that at early epochs ($0.5 < z < 3$) about 70% of the co-moving star formation rate density (SFRD) is obscured by dust (Chary & Elbaz 2001). This refocused the main approaches of galaxy formation studies, since it high-lightened the strict need of parallel FIR observations to fully characterize galaxy evolution. An important challenge for such studies is the low resolution of commonly used FIR and sub-mm instruments, such as Herschel (beams or 4-10 arcsec) and single-dish sub-millimeter telescopes (beams of 1–4 arcmin), thus with high-changes of confusion, e.g., measuring several sources blended within one resolution element. This challenge has been overcome thanks to de-blending approaches using prior knowledge from higher-resolution observations at related wavelengths, such as 24 μm priors, or radio interferometric observations, and especially thanks to the advent of new sub-mm interferometers such as ALMA.

Black-hole accretion has been observed to be in great part obscured by dust and gas as well, however the origin of AGN obscuration is less well understood and is still a source of debate in the extragalactic community. Historically, AGN obscuration was thought to be an inclination effect, based on detections of polarized broad lines in obscured sources (Antonucci & Miller 1985). Since the obscuring material is assumed to be distributed in the shape of a torus, the obscured fraction would therefore be determined by the viewing angle; while a face-on view would allow a direct glimpse into the accretion disk and broad line region, producing an unobscured AGN or Type 1, an edge-on view would observe the AGN through the toroidal structure that would cover the broad line region, producing an obscured or Type 2 AGN. While it is widely accepted that AGN obscuration is produced in part by inclination, it has been shown that obscuration is a more complex phenomenon. Luminosity is known to

play an important role, where more luminous objects have been observed to be less obscured by being capable of pushing the obscuring medium by radiation pressure (receeding torus model Ricci et al. 2017). Evolutionary models of massive galaxies suggest that obscuration in AGN would be related to a short phase, right after a starburst event, assuming that both star formation and AGN activity are promoted by a galaxy merger event (Hopkins et al. 2008). Obscuration by dust and gas plays a fundamental role in galaxy and black-hole evolution across cosmic history. Chapters 2 and 5 will explore in depth this property for AGN and star forming galaxies, respectively.

Extreme sources

The increase of the galaxy 'main sequence' as a function of redshift, implies that at a given stellar mass, the star formation rates expected for 'typical' galaxies can increase by a factor 20 when going from $z = 0$ towards the peak at $z \sim 2$ (Sargent et al. 2012). Therefore, the most spectacular and extreme sources in both star formation and black-hole accretion are more likely to be found at $z \sim 2$. Here, I will shortly present some of the galaxy populations investigated in this thesis.

Active Galactic Nuclei (AGN): The AGN phenomenon is a complex concept since although AGNs are generally defined as accreting black-holes hosted in galaxy centers, this definition might apply as well for galaxies with small black-hole masses or accretion rates so low, that the intrinsic emission is not detectable or outshone by the host galaxy emission. In this thesis, by AGN are generally meant nuclear sources with bolometric luminosities from $L_{bol} \sim 10^{41} - 10^{48}$ erg s^{-1}and black-hole masses of a few $10^6 - 10^{10}$ $M_\odot$. Since historically all galaxies and AGN have been classified by their observational characteristics rather than their physical ones, some of the most common AGN types are: *Seyfert galaxies type 1 and 2*, the most common unobscured and obscured AGN in the local Universe, respectively; *radio galaxies*, bright radio sources typically associated with large relativistic jets (see disambiguation with radio-selected galaxy below); and *quasars*, the most luminous distant continuously-emitting sources in the early Universe. Although all these sources present overlaps in their intrinsic properties, and the different mass bins and redshifts probed might be the main source of diversity, the question whether other fundamental physical differences exist among them is still a matter of discussion. In this thesis, we will explore this question and recover physical intrinsic properties by modelling their multiwavelength emission. The second and third chapter of this thesis focus on AGN of two different selections: X-ray selected AGN and radio selected AGN, respectively. Both AGN populations cover redshift ranges of $z = 0.5 - 2.5$, including Seyfert 1 and 2; radio AGN; and QSO 1 and 2.

Dusty star-forming galaxies (DSFGs), starbursts, and submillimeter galaxies (SMGs):

Star-forming galaxies have been classified into several types based on their selection, which can sometimes be confusing due to the large overlap of the intrinsic physical properties of these classes. A large population of star forming galaxies, key in the phase of galaxy assembly, are dusty star forming galaxies (DSFGs, Casey et al. 2014). DSFGs are generally defined to be galaxies with prominent infrared emission and large amount of dust attenuation. As explained in Section 1.3, DSFGs likely represent the majority of star forming galaxies since dust distributions are a main by-product of the star formation process itself. These galaxies are sometimes also referred to as starburst galaxies, which have however a more strict definition: their star formation histories are characterized by short-lived intense periods of star formation; and they lay above the main sequence, forming a second component in the SFR-M* plot with a factor 4 to 10 times higher star formation rates than galaxies on the main sequence. Early observations with infrared telescopes have detected such galaxies in the local Universe and called them ultra-luminous (ULIRGs, $\log(\mathrm{LIR}[L_\odot]) \geq 12$) and luminous

(LIRGs, $11 \leq \log(\mathrm{LIR}[L_\odot]) \leq 12$) infrared galaxies, where LIR is the total IR luminosity from $8 - 1000\ \mu$m (see Sanders & Mirabel 1996, for a review). *Sub-millimeter galaxies* are interesting DSFGs at high redshift, defined as galaxies strongly detected by sub-mm instruments. SMGs were initially discovered in the late 1990s with the SCUBA[4] and MAMBO[5] instruments. Due to the shift of the FIR SED to sub-mm wavelengths, the redshift distribution of SMGs is centered at $z \sim 2$. It is important to note, that although SMGs are highly star-forming and originally considered to strictly lay above the main sequence, some of the most massive SMGs may actually be main sequence galaxies due to their large masses at $z \sim 2$.

Radio-selected galaxies, were historically defined as a class of AGNs, since the low sensitivity of radio telescopes, before the advent of radio interferometres, probed almost exclusively AGN-originated radio emission. However, as discusses in Section 1.2, the increasing sensitivity of radio telescopes (such as the VLA and LOFAR) has started to probe lower luminosities, largely populated by star forming galaxies. Chapter 3 in thesis studies as well a sample of radio-selected star forming galaxies, which at high redshifts imply star-forming galaxies of SFR$> 500\ M_\odot$/yr given the sensitivity of the instruments used.

1.4 This Thesis

This thesis presents pioneering work on the panchromatic emission of some of the most luminous sources in the early Universe: star forming galaxies and active galactic nuclei. Using state-of-the-art statistical methods and new-generation radio-to-optical instruments, this thesis builds up on the current knowledge presented above to expand the parameter space covered by current multi-wavelength studies. In particular, this thesis pushes three different frontiers: the statistical frontier, the wavelength frontier and the resolution frontier. This study focuses on star-forming galaxies, AGN and composite galaxies at redshifts $z \sim 1 - 3$, all with rich ancillary multi-wavelength coverage from the radio-to-X-rays.

In **Chapter 2** we push **the statistical frontier** by exploring the complex parameter spaces needed to model the multiwavelength emission of galaxies and their AGN. In particular, we developed the probabilistic tool AGN*fitter* to consistently model the panchromatic emission of galaxies and accreting black-holes using physical semi-empirical and theoretical models from the UV to the sub-millimetre. We explore the statistical challenges associated with sampling such a complex parameter space, prone to correlations and degeneracies, and address these challenges by using a sophisticated Bayesian approach based on the Markov Chain Monte Carlo method. We apply the code to study the panchromatic emission of X-ray selected obscured and unobscured AGN from the COSMOS field. In this chapter, we show that our method is able to recover the entire probability density functions, including the mean values and, most crucially, the uncertainties of all physical parameters, such as stellar masses, star formation rates, AGN bolometric luminosities, reddening parameters, AGN obscuration, and AGN fraction. Finally, we test the capability of our multi-wavelength SED-fitting tool to recover the obscuration properties of the nuclear AGN region through comparisons with optical spectroscopy. Despite the ~7 order of magnitude difference between the scales probed by the AGN and those of the integrated galaxy emission, we show that AGN*fitter* is able to robustly classify the AGN into obscured and unobscured AGN by modelling the photometric data with 80% reliability. These results were presented in Calistro-Rivera et al. (2016).

In **Chapter 3** we push **the wavelength frontier** and present the first galaxy and AGN

[4]Sub-millimetre Common User Bolometer Array
[5]MAx-Planck Millimetre BOlometer

evolution study, as seen from the new frequency window opened by the Low Frequency ARray (LOFAR). Thanks to the combination of resolution and sensitivity achieved by LOFAR, we are able to build an unprecedented statistical sample of low-frequency radio-selected galaxies and AGN till redshifts of $z \sim 2.5$. We connect the low-frequency radio emission at 150 MHz to the FIR-UV SED by reconstructing the radio SED from low-to-high frequencies, using ancillary radio data, and by applying the method presented in Chapter 2 to reconstruct the panchromatic SED. We build the deepest sample of radio SEDs of galaxies and AGN from low-to-high frequencies, finding a significant difference in the shapes of the star-formation (SF) dominated sources as compared to the AGN-dominated ones, where the SF dominated galaxies tend to flatten towards lower frequencies. Focussing on the sub-sample of star forming galaxies, in this chapter we investigate for the first time the far-infrared-radio correlation for the low-frequency radio. Our results suggest that the FIR-radio correlation at high and low frequencies is not constant as suggested by previous literature, but evolve as a function of redshift. Finally, we present the first calibration of the radio emission at 150 MHz as a star-formation tracer, and provide a fitting function for the radio-SFR relation at 150 MHz. These results were presented in Calistro-Rivera et al. (2017).

In **Chapter 4** we push **the resolution frontier** by studying the multiwavelength emission at subarsecond resolution of four dusty star-forming galaxies at $z \sim 2-3$, selected in the sub-millimeter regime. Exploiting the unparalleled combination of depth and resolution of the ALMA interferometer, together with imaging from the *Hubble Space Telescope* (*HST*), we investigate the spatial and physical properties of the insterstellar medium, as seen from the molecular gas and dust continuum emission, and of the stellar emission of these galaxies. We observe the molecular gas as traced by the ^{12}CO($J = 3-2$) emission, and investigate the dynamical properties of the galaxies based on kinematic modelling, finding that these sources are consistent with disk rotation to first order. The high-resolution multiwavelength emission shows that the resolved spatial distributions of the dust continuum emission and, most remarkably, the molecular gas emission, can both be entirely offset to the stellar emission.We apply a statistical analysis of the observed sizes based on stacking of the molecular gas, dust continuum and stellar emission components of a larger sample of dusty star forming galaxies. We find that the cool molecular gas emission in these sources (radii$\sim 5-14$ kpc) is clearly more extended than the rest-frame ~ 250 μm dust continuum by a factor > 2. Assuming a constant dust-to-gas ratio, we find that this apparent difference in sizes can be explained by temperature and optical-depth gradients alone. The results of this chapter suggest that caution must be exercised when extrapolating morphological properties of dust continuum observations to conclusions about the molecular gas phase of the ISM. These results were presented in Calistro-Rivera et al. (2018).

In **Chapter 5** we complement the study of the interstellar medium at high resolution presented in Chapter 4, by studying the [C II] emission of two of the dusty star-forming galaxies in our previous sample. In particular, we compare ALMA measurements of gas emission line [C II] at 0.15 arcsecond resolution to the cool molecular gas emission traced by the ^{12}CO($J = 3-2$), presented above. We find that the [C II] surface brightness distribution is dominated by a compact core $\sim$1 kpc in radius, a factor of 2–3 smaller than the CO (3–2) emission, embedded in an extended, low surface-brightness [C II] component. We find that galaxies exhibit a strong [C II]/FIR deficit, with FIR surface brightness–[C II]/FIR slope steeper than in local star-forming galaxies. We compare our [C II]/CO(3–2) observations from Chapter 4 and 5 with PDR models, finding that a strong FUV radiation field ($G_0 \sim 10^4$) and moderate density (n(H) $\sim 10^3$ cm^{-3}) in the centre of the galaxies. We find that the pronounced [C II]/FIR deficit in these sources is probably a thermal saturation of the C$^+$ fine-structure lev-

els, and a significantly reduced heating of the gas via the photoelectric effect. These results have been submitted and will be presented in Rybak, Calistro-Rivera et al. (2018)[6].

[6]This chapter is part of this PhD Thesis due to my significant contribution to this project at all levels. The main result of this chapter is based on the comparison of the [C II] data to the CO observations presented in Chapter. I have been active in both the realization and discussion of this comparative analysis. Additionally, I have carried out the kinematic modelling of the [C II] data presented in section 2.3 and have written the description of the process in this chapter. Finally, I have proof-read and edited different versions of this chapter, and have led the ALMA Cycle 4 proposal to complete the [C II] observations for the two remaining sources from Calistro-Rivera et al. (2018).

Bibliography

Aird, J., Coil, A. L., & Georgakakis, A. 2018, MNRAS, 474, 1225

Aird, J., Coil, A. L., Georgakakis, A., et al. 2015, MNRAS, 451, 1892

Alonso-Herrero, A., Ramos Almeida, C., Mason, R., et al. 2011, ApJ, 736, 82

Antonucci, R. R. J., & Miller, J. S. 1985, ApJ, 297, 621

Bolzonella, M., Miralles, J.-M., & Pelló, R. 2000, A&A, 363, 476

Brandt, W. N., & Alexander, D. M. 2015, A&A Rev., 23, 1

Brinchmann, J., Charlot, S., White, S. D. M., et al. 2004, MNRAS, 351, 1151

Brinchmann, J., & Ellis, R. S. 2000, ApJ, 536, L77

Burgarella, D., Buat, V., & Iglesias-Páramo, J. 2005, MNRAS, 360, 1413

Carilli, C. L., & Walter, F. 2013, ARA&A, 51, 105

Casey, C. M., Narayanan, D., & Cooray, A. 2014, Phys. Rep., 541, 45

Condon, J. J. 1992, ARA&A, 30, 575

Conroy, C. 2013, ARA&A, 51, 393

Conselice, C. J., Wilkinson, A., Duncan, K., & Mortlock, A. 2016, ApJ, 830, 83

da Cunha, E., Charlot, S., & Elbaz, D. 2008, MNRAS, 388, 1595

Einstein, A. 1916, Annalen der Physik, 354, 769

Gaia Collaboration, Brown, A. G. A., Vallenari, A., et al. 2018, A&A, 616, A1

Gültekin, K., Richstone, D. O., Gebhardt, K., et al. 2009, ApJ, 698, 198

Harris, G. L. H., Rejkuba, M., & Harris, W. E. 2010, Publications of the Astronomical Society of Australia, 27, 457

Hopkins, P. F., Hernquist, L., Cox, T. J., & Kereš, D. 2008, ApJS, 175, 356

Ichikawa, K., Packham, C., Ramos Almeida, C., et al. 2015, ApJ, 803, 57

Kirkpatrick, A., Pope, A., Alexander, D. M., et al. 2012, ApJ, 759, 139

Kormendy, J., & Richstone, D. 1995, ARA&A, 33, 581

Lynden-Bell, D. 1969, Nature, 223, 690

Lynden-Bell, D., & Rees, M. J. 1971, MNRAS, 152, 461

Madau, P., & Dickinson, M. 2014, ARA&A, 52, 415

Magorrian, J., Tremaine, S., Richstone, D., et al. 1998, AJ, 115, 2285

Marconi, A., & Hunt, L. K. 2003, ApJ, 589, L21

Muzzin, A., Marchesini, D., van Dokkum, P. G., et al. 2009, ApJ, 701, 1839

Nenkova, M., Ivezić, Ž., & Elitzur, M. 2002, ApJ, 570, L9

Padovani, P. 2016, A&A Rev., 24, 13

Perlmutter, S., Aldering, G., Goldhaber, G., et al. 1999, ApJ, 517, 565

Planck Collaboration, Ade, P. A. R., Aghanim, N., et al. 2014, A&A, 571, A16

Rejkuba, M., Harris, W. E., Greggio, L., & Harris, G. L. H. 2011, A&A, 526, A123

Ricci, C., Trakhtenbrot, B., Koss, M. J., et al. 2017, Nature, 549, 488

Riess, A. G., Filippenko, A. V., Challis, P., et al. 1998, AJ, 116, 1009

Rosario, D. J., Trakhtenbrot, B., Lutz, D., et al. 2013, A&A, 560, A72

Rosario, D. J., McIntosh, D. H., van der Wel, A., et al. 2015, A&A, 573, A85

Sanders, D. B., & Mirabel, I. F. 1996, ARA&A, 34, 749

Sargent, M. T., Béthermin, M., Daddi, E., & Elbaz, D. 2012, ApJ, 747, L31

Schmidt, M. 1963, Nature, 197, 1040

Seyfert, C. K. 1943, ApJ, 97, 28

Shakura, N. I., & Sunyaev, R. A. 1973, A&A, 24, 337

Smail, I., Swinbank, A. M., Ivison, R. J., & Ibar, E. 2011, MNRAS, 414, L95

Tielens, A. G. G. M. 2008, ARA&A, 46, 289

Volonteri, M., Capelo, P. R., Netzer, H., et al. 2015, MNRAS, 449, 1470

Whitaker, K. E., van Dokkum, P. G., Brammer, G., & Franx, M. 2012, ApJ, 754, L29